PAMM

SPECIAL ISSUE 95th Annual Meeting of the International Association of Applied Mathematics and Mechanics (GAMM)

RESEARCH ARTICLE OPEN ACCESS

Wave Propagation in Non-Uniform Media by Linear Expansion of the Refraction Law

Alessandro Bassetti[1] | Oskar Bschorr[2]

[1]TUHH, Hamburg University of Technology, Structural Mechanics in Lightweight Design, Acoustics, Hamburg, Germany | [2]Aeroakustik Stuttgart

Correspondence: Alessandro Bassetti (alessandro.bassetti@tuhh.de)

Received: 25 September 2025 | **Accepted:** 17 November 2025

ABSTRACT

The propagation of mechanical waves in an unbounded, non-uniform medium can be described by using curvilinear coordinates centered at the source position. The Frenet coordinate system, with origin on a point riding a wave, is used as a basis for the curvilinear coordinates. In this way a principal coordinate stating the evolution of the wave field and running along a ray, orthogonally to the successive wave fronts, is determined. A linear expansion of the refraction law at the rider point connects the gradient of the speed of sound field to the curvatures of the wave path and of the wave front. We use this connection in developing a numerical solution for the wave field, after recalling recent developments about the historical determination of the refraction law.

1 | Introduction

The law of refraction stems from optics, and it is known as Snell's law, after the name of Willebrord Snellius, commonly known as Snell. Snellius is the Dutch astronomer and mathematician who first discovered and effectively communicated the refraction law to the current scientific community. Even if Snellius did not officially publish his work, his discovery has been noted by contemporary scientists and named after him. One of the manuscripts by Snellius has been recently translated from Latin to German by Hentschel [1]. In ref. [1] the attempt is made to reconstruct the way Snellius took toward his discovery of the refraction law. Today we know that Snellius was not the first to discover the law. Thomas Harriot preceded Snellius in this discovery, but his notes on the topic, see ref. [2], were kept unpublished and were not communicated until after his dead. They have been recovered after the work of Snellius had been acknowledged. As reported by Rasched [3], the discovery and communication of the refraction law had happened over 600 years before Snellius, within the court of Baghdad. Ibn Sahl fully described the law of refraction in his treatise "On the Burning Instruments," which was written around the Year 984. We can then state that the refraction law has been independently discovered at least three times.

The refraction law can be derived from Fermat's principle of minimum propagation time. It can also be deduced by using the Huygens principle on the evolution of wave fronts in two media separated by a planar boundary. Also, a phase speed matching for the waves in the two media and along the planar separation boundary outputs the refraction law. The law is valid for all types of waves: for longitudinal and transverse mechanical waves in solids and for sound waves in fluids, as well as for electromagnetic waves. It can be represented as indicated in the diagram in Figure 1, where the incidence and refraction angles α_1 and α_2 are related by Equation (1).

$$\frac{\sin\alpha_1}{c_1} = \frac{\sin\alpha_2}{c_2} \tag{1}$$

In the present work, we use the refraction law to approach wave propagation in inhomogeneous media. The scattering problem associated with the refraction at a plane between two media having a propagation-speed discontinuity is adapted to ray acoustics

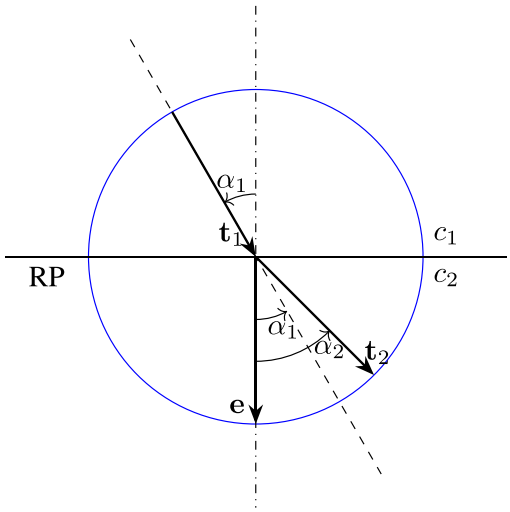

FIGURE 1 | Diagram representing the refraction path in the scattering problem associated with wave propagation through a rectilinear interface RP, between two media with different wave-propagation speeds c_1 and c_2. A unit-radius circle is reported in blue, to indicate that the three vectors in the diagram are unit vectors. The circle is centered on the point in which the incident field, propagating along $\mathbf{t}_1$, encounters the interface plane. The unit vectors represent the incident- and refracted-field propagation directions, $\mathbf{t}_1$ and $\mathbf{t}_2$, and the normal of the interface plane, $\mathbf{e}$. Note that $\mathbf{e}$ points the medium at higher propagation speed. The incidence ($i = 1$) and refraction ($i = 2$) angles α_i are the angles between $\mathbf{e}$ and $\mathbf{t}_i$.

in a medium with a continuous field for the wave propagation speed. The problem considers dynamics with a single type of wave (we do not consider the co-existence of different wave dynamics such as shear and longitudinal waves in solid continua), and it is limited to the kinematics of the wave propagation. In this situation, as proposed by Bschorr [4], one can use the refraction law locally, in order to define the wave path connecting a source and an observation point in the medium. Bschorr and Bassetti [5] formulated the theory by Bschorr, linking it to curvilinear coordinates evolving with the wave path. They also proposed an extension of the theory, in which the local-refraction approach is used to determine the evolution of the curvature of the wave front, together with the wave path. We are publishing here a short review the theory by Bschorr and Bassetti and an application example inspired by an old experiment on sound propagation in the atmosphere. The old experiment has been reported by Gabrielson [6] as an example of sound propagation in the atmosphere in which, due to refraction, sound was perceived at unusually long distances from the source while not being perceived in some areas lying closer to the sound source.

2 | On Sound Propagation in a Medium With Continuous Wave Propagation Speed

The present analysis is based on an inhomogeneous, isotropic medium that is unlimited on all sides. The wave-propagation speed, characteristic of the medium, is a scalar field defined as a function of the global Cartesian coordinates (x, y, z), such that $c = c(x, y, z)$. We assume $c = c(x, y, z)$ as continuous function, with defined gradient $\nabla c = \nabla c(x, y, z)$ at any point. For a given distribution of c, see the exemplary distribution in Figure 2a, ∇c lies orthogonally to the contour lines of c, pointing the side of the contour line toward greater values of c. By assuming the radius of curvature of the contour lines is much greater than the wavelength associated with an incident wave field, the refraction of the incident field can be worked out locally. This is done by applying the refraction law, Figure 1 and Equation (1), with the interface RP assumed to be the tangent plane at the incidence point and with an infinitesimal variation dc of the wave-propagation speed, see Figure 2a,b. In this situation, the refraction law 1 can be reduced to its linear expansion, due to the infinitesimal variation of the incidence through the continuous speed of sound field:

$$\frac{\sin\alpha}{c} = \frac{\sin(\alpha + \mathrm{d}\alpha)}{c + \mathrm{d}c} = \frac{\sin\alpha + \mathrm{d}\alpha\cos\alpha}{c + \mathrm{d}c} \Rightarrow \mathrm{d}\alpha = \frac{\sin\alpha}{\cos\alpha}\frac{\mathrm{d}c}{c} \quad (2)$$

We note that Equation (2) directly connects a variation of the propagation speed c to a rotation of the wave path. The assumed continuity of c has then the implication that the wave paths in the given medium are curved lines whose tangential direction rotates smoothly by following the variations of a continuous function. This fact induces the introduction of a curvilinear coordinate system, which can be associated with radiation from a point source and the speed of sound distribution across the medium. For an arbitrary point P, indicating the position of an infinitesimally small wave surfer, see Figure 3, who moves along the curved wave path at the speed c, we can define a Frenet reference system including the orthogonal unit vectors $\mathbf{t}$, $\mathbf{n}$, and $\mathbf{b}$. If we define a metric along the wave path, red curve in Figure 3, we have a new coordinate ξ that measures the distance traveled from the point source on the wave path by the wave surfer, connected to the wave front. The unit vectors of the Frenet reference are defined as follows:

$$\begin{aligned} \mathbf{t} &= \frac{\mathrm{d}P}{\mathrm{d}\xi} \\ \mathbf{n} &= R_\xi \frac{\mathrm{d}\mathbf{t}}{\mathrm{d}\xi} \\ \mathbf{b} &= \mathbf{t} \times \mathbf{n} \end{aligned} \quad (3)$$

The unit vector $\mathbf{t}$ is locally orthogonal to the wave front, in other words, it is the unit normal to the wave-front tangent plane (WFP), pointing toward the wave propagation. The unit vector $\mathbf{n}$ is in the local osculating plane of the wave path, spanned by $\mathbf{t}$ and ∇c, and it is defined in terms of the curvature radius R_ξ of the wave path in P. A further definition of $\mathbf{n}$ can be made by decomposing the speed of sound gradient ∇c into two vector components, lying parallel and orthogonal to the unit vector $\mathbf{t}$. In this case we note that the vectorial component perpendicular to $\mathbf{t}$ always lies opposite to $\mathbf{n}$. This can be deduced from the diagram in Figure 4a, drawn on the osculating plane for $0 < \alpha < \pi/2$. For the α in Figure 4a, the increment dα must be positive, according to the refraction laws Equations (1) and (2). In Figure 4a, the projections of ∇c along the directions parallel and perpendicular to $\mathbf{t}$ have amplitudes given as:

$$\left|\nabla_{/\!/} c\right| = |\nabla c|\cos\alpha \qquad \text{and} \qquad |\nabla_\perp c| = |\nabla c|\sin\alpha \quad (4)$$

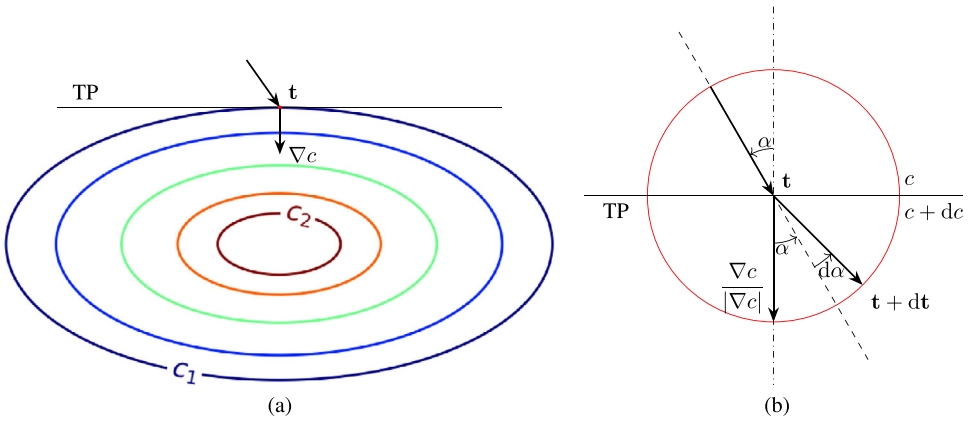

FIGURE 2 | (a) Continuous wave propagation field $c(x, y, z)$ with contour lines for c in a region of variability of the propagation speed, between the values c_1 and c_2, with $c_1 < c_2$. The gradient ∇c is reported at a point in the field, together with the tangent plane (TP) to the local contour line. (b) Local refraction process in the vicinity of a point in the field, where the local tangent plane serves as refraction plane and an infinitesimal rotation of the tangent vector $\mathbf{t}$ corresponds to an infinitesimal increment of the propagation speed.

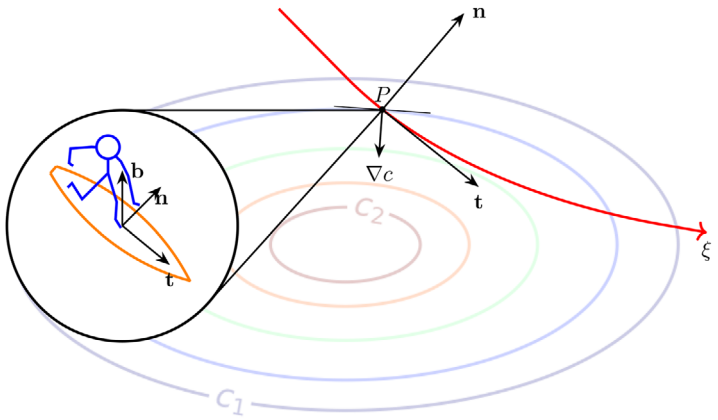

FIGURE 3 | An infinitesimally small surfer is tracked on the wave path at the position P. The corresponding Frenet basis of vectors, Equation (3), is sketched in the diagram with the surfer, where the binormal $\mathbf{b}$ is out of the plane of the 2D diagram on the osculating plane. The osculating plane is spanned by $\mathbf{b}$ and ∇c.

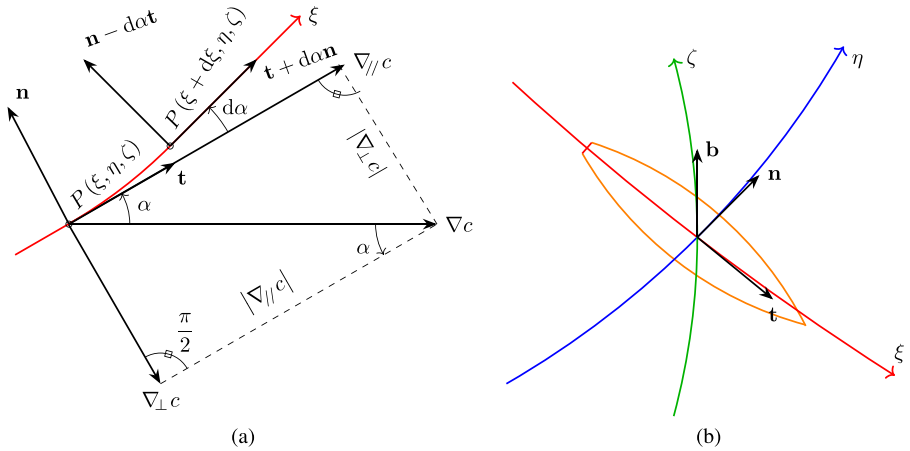

FIGURE 4 | (a) Decomposition of the propagation-speed gradient ∇c along and perpendicularly to the radiation direction $\mathbf{t}$. The evolution of $\mathbf{t}$ and $\mathbf{n}$ over an increment of curvilinear coordinate ξ is also visualized. Note the fact that $\mathbf{n}$ lies opposite to the vector $\nabla_\perp c$ at any given curvilinear coordinate ξ. (b) Wave path at an arbitrary point in space, with corresponding Frenet reference frame and the coordinate lines η and ζ, spanning the local approximating circles of the wavefront in the osculating and longitudinal planes, respectively.

The result for the vectorial components and the further definition of **n** follow as:

$$\nabla c = \nabla_{/\!/} c + \nabla_{\perp} c = (|\nabla c| \cos\alpha)\,\mathbf{t} - (|\nabla c| \sin\alpha)\,\mathbf{n} \quad \text{and} \quad \mathbf{n} = -\frac{\nabla_{\perp} c}{|\nabla_{\perp} c|} \tag{5}$$

As we will state in Section 3, the above expression can be used to determine the curvature radius of the wave path R_ξ as a function of the wave propagation speed c, its gradient ∇c, and the local incidence angle α.

3 | The Curvature Radii Along and Perpendicularly to the Wave Path

For each wave path from a source in the given medium, it is possible to define a curvilinear coordinate ξ expressing the distance from the source traveled by an infinitesimal portion of the wavefront along the path. The wavefront in the vicinity of the wave path can be described by the curvilinear coordinates η, along **n**, and ζ, along **b**. In Figure 4b we report the wave path in red and the intersections of the local wave front in blue and green. These intersections are the one between the wavefront and the osculating plane, spanned by **n** and **t**, which is represented in blue, and the one the wavefront has with the longitudinal plane, spanned by **b** and **t**, which is represented in green. Their metrics around the wave path are respectively given by the coordinates η and ζ, with origin on the wave path. In the present section, we derive the radii of curvature for the wave path and the two circles that approximate the wavefront intersections with the osculating and longitudinal planes. The curvature radii are indicated here as R_ξ, R_η, and R_ζ according to the curvilinear coordinate on the respective curve. The results can be found in ref. [5], where we used a different notation, which is related to the one in the present work as follows:

$$R \to R_\xi \qquad r \to R_\eta \qquad r_\zeta \to R_\zeta$$

3.1 | Curvature of the Wave Path

For a general curve with a metric ξ, one can state that the increment of the tangent vector **t** is aligned with the normal **n**. As a consequence, for non-zero increments of **t** at varying curvilinear coordinate ξ, one can state

$$\mathbf{n} = \frac{1}{\left|\frac{\mathrm{d}\mathbf{t}}{\mathrm{d}\xi}\right|}\frac{\mathrm{d}\mathbf{t}}{\mathrm{d}\xi} \tag{6}$$

By comparing Equation (6) to the Frenet definition of **n** in Equation (3), we can express the curvature radius of the wave path as

$$R_\xi = \left|\frac{\mathrm{d}\xi}{\mathrm{d}\mathbf{t}}\right| = \left|\frac{\mathrm{d}\xi}{\mathbf{n}\mathrm{d}\alpha}\right| = \left|\frac{\mathrm{d}\xi}{\mathrm{d}\alpha}\right| \tag{7}$$

where we used the fact that $|\mathbf{n}| = 1$. By using Equation (2), to express the increment of incidence $\mathrm{d}\alpha$, we obtain

$$R_\xi = \left|\frac{c\mathrm{d}\xi\cos\alpha}{\sin\alpha \mathrm{d}c}\right| = \left|\frac{c\mathrm{d}\xi\cos\alpha}{\sin\alpha \nabla c\cdot\mathbf{t}\mathrm{d}\xi}\right| = \left|\frac{c\cos\alpha}{\sin\alpha|\nabla c|\cos\alpha}\right| = \frac{c}{|\sin\alpha|\,|\nabla c|} = \frac{c}{|\nabla_\perp c|} \tag{8}$$

Equation (8) is an expression of the radius of curvature of the wave path as a function of the wave-speed distribution and of the incidence α between the wave-speed gradient ∇c and the tangent vector **t** to the wave path. In ref. [5] we offer an alternative derivation of Equation (8), still combining the linear expansion of the refraction law and considerations on a curved trajectory. An analogous expression is given in Section "3.8" of ref. [7], where the curvature of the wave path is established by using a different approach.

3.2 | Curvatures of the Wavefront at the Wave Path

In a homogeneous medium, the wavefronts are spherical surfaces, and the wave path is rectilinear. In that case the distance traveled by any point P, with coordinates $[x, y, z]$, on the wavefront from the source S, with coordinates [0,0,0], is identical to the distance from the source; it also corresponds to the curvature radius of the wavefront:

$$r = \sqrt{x^2 + y^2 + z^2} = R_\eta = R_\zeta$$

In the present situation, with an inhomogeneous wave speed field $c(x, y, z)$, the distance traveled by a point on the wavefront from the source is given by the coordinate ξ, and the curvature radii of the wavefront are no more related to the coordinate ξ or to the distance r. The wavefront lies orthogonal to the wave path and is locally spanned by the curvilinear coordinates η and ζ, with origin on the wave path. The intersections of the wavefront with the osculating and the longitudinal planes can be approximated with circles of radii R_η and R_ζ centered at curvature centers S and Z. In Figure 5 we report the local refraction in the osculating plane (a) and in the longitudinal plane (b). We also sketch the variation of the curvature radii R_η and R_ζ due to an increment $\mathrm{d}c$ of the wave speed. As reported in ref. [5], the variation of R_η at varying curvilinear coordinate along the wave path can be expressed as follows:

$$\frac{\mathrm{d}R_\eta}{\mathrm{d}\xi} = 1 - \mathrm{B}(\alpha)\,\frac{R_\eta}{c}\nabla c\cdot\mathbf{t} \tag{9}$$

In Equation (9) the positive factor $\mathrm{B}(\alpha)$ is defined as

$$\mathrm{B}(\alpha) = \frac{1 + (\sin\alpha)^2}{(\cos\alpha)^2} \tag{10}$$

The evolution of R_η along a wave path is obtained by integrating Equation (9) from the source to the desired position on the path:

$$R_\eta = \int_0^\xi \left(1 - R_\eta \mathrm{B}(\alpha)\frac{\nabla c\cdot\mathbf{t}}{c}\right)\mathrm{d}\xi \tag{11}$$

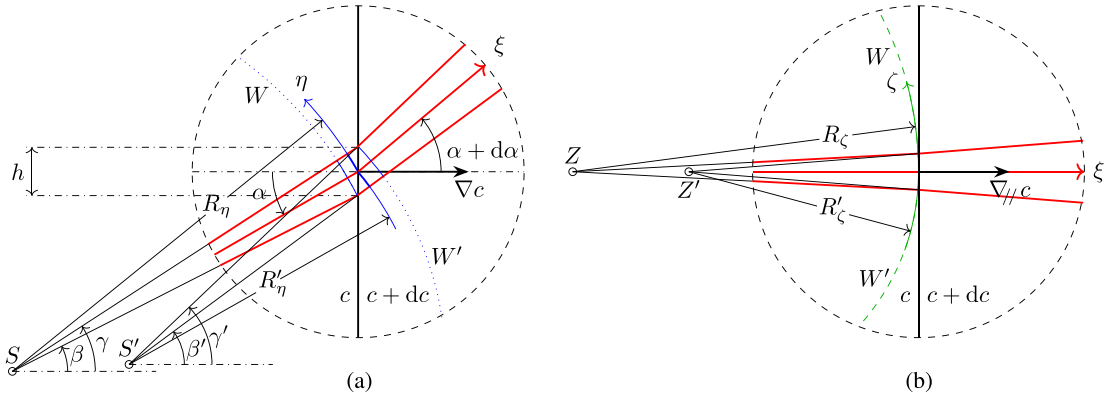

FIGURE 5 | Evolution of the wavefront curvature radii through a local refraction process in the osculating plane (a) and in the longitudinal plane (b). Quantities after refraction are indicated with primed symbols. Note that the representation in (b) results from a negative rotation of the quantities in (a) around $\mathbf{t}$ and with an amplitude of a fourth of a full turn. The component $\nabla_{//}c$ of ∇c is orthogonal to the intersection between the refraction plane and the longitudinal plane, reported in (b) and denoting the transition line for the propagation speed.

The curvature variation of the wavefront intersection with the longitudinal plane is easily deduced by specializing Equation (9) to the situation represented in Figure 5b, where the factor $\mathrm{B}(0) = \mathrm{B}(\pi) = 1$ and the component $\nabla_{//}c$, of the wave-speed gradient parallel to $\mathbf{t}$, must be used in place of ∇c.

$$\frac{\mathrm{d}R_\zeta}{\mathrm{d}\xi} = 1 - \frac{R_\zeta}{c}\nabla_{//}c \cdot \mathbf{t} \tag{12}$$

The evolution along the path of the longitudinal-plane wavefront curvature is expressed as follows:

$$R_\zeta = \int_0^\xi \left(1 - R_\zeta \frac{\nabla_{//}c \cdot \mathbf{t}}{c}\right) \mathrm{d}\xi \tag{13}$$

4 | Anomalous Sound Propagation Between Berlin and Poznan

The present section applies the linearized refraction model to numerically trace sound waves in a stratified atmosphere. As explained in ref. [5], the standard atmosphere defined in ref. [8] by the International Civil Aviation Organization (ICAO) can be easily used as medium for the present theory. An example of anomalous sound propagation has been reported by Gabrielson [6]: an experiment made in December 1925, in the German Empire, resulted in a pattern of zones across the empire where a loud explosion in a firing range southwest of Berlin could be heard. The city of Poznan, hosting the 2025 GAMM conference, was part of the experiment as observation point. The city Frankfurt Oder is located roughly on the geodesic line between the explosion site and Poznan. The geodesic distances from the explosion site to the cities Frankfurt Oder and Poznan are approximately 90 and 250 km, respectively. Nevertheless, the explosion sound was heard in Poznan but not in Frankfurt Oder.[1] This result is a consequence of the refraction in the atmosphere due to its temperature or sound speed variation with the altitude above the ground. In the troposphere we normally have decreasing temperature at growing height. This means that sound emitted from a source on the ground radiates along a path, which is bent upward. In the stratosphere, we have a temperature gradient aligned with growing altitude, and this bends the sound path downward. The full result of the explosion audibility experiment is shown in Figure 6: a pattern of audibility regions was observed as distorted rings placed around the firing range. As Gabrielson [6] pointed out, such a pattern is the result of the temperature distribution in the atmosphere. The ring-shaped patterns of audibility alternating with zones of silence indicated a strong refraction of sound in the stratosphere and the reflection on ground as being responsible for the special sound radiation on that day. In ref. [5], we noted that by applying the standard profile of the ICAO standard atmosphere, we can explain a zone of silence in the vicinity of the source on the ground, which we called the antisphere of silence. The stratosphere of the ICAO standard atmosphere induces a negative curvature on the sound paths but is not sufficient to bend them back toward the ground. By looking at the winter profile of atmospheric temperatures presented in Figure 11 of ref. [6], we noted a much warmer stratosphere than in the standard atmosphere. We adapted the temperature values of the piecewise linear temperature profile we used for the standard atmosphere in order to have conditions that are closer to the experiment ones. The resulting temperature and speed of sound profiles are in Figure 7a. In Figure 7b, we report the numerical evaluation, detailed in ref. [5], of sound paths from a source on the ground, up to a maximum altitude of 60 km or down to the ground. The sound paths are calculated for 31 equispaced initial polar angles, spanning the interval $[0, \pi/2)$ rad from the normal to the ground. For the given atmospheric temperature profile, the radiation sphere has a diameter of 240 km, and the corresponding antisphere of silence is reported in Figure 7b as the gray region in the troposphere, lying below the sound path at the largest initial polar angle. The refraction effect due to the speed of sound gradient in the stratosphere bends a considerable part of the radiated sound back to the ground: according to Figure 7b, rays departing the source at polar angles wider than 64.5° come back to the ground, and this corresponds to 43% of the radiated sound energy, assuming a non-directional source and without considering atmospheric losses. To summarize, in spite of using an extremely simplified

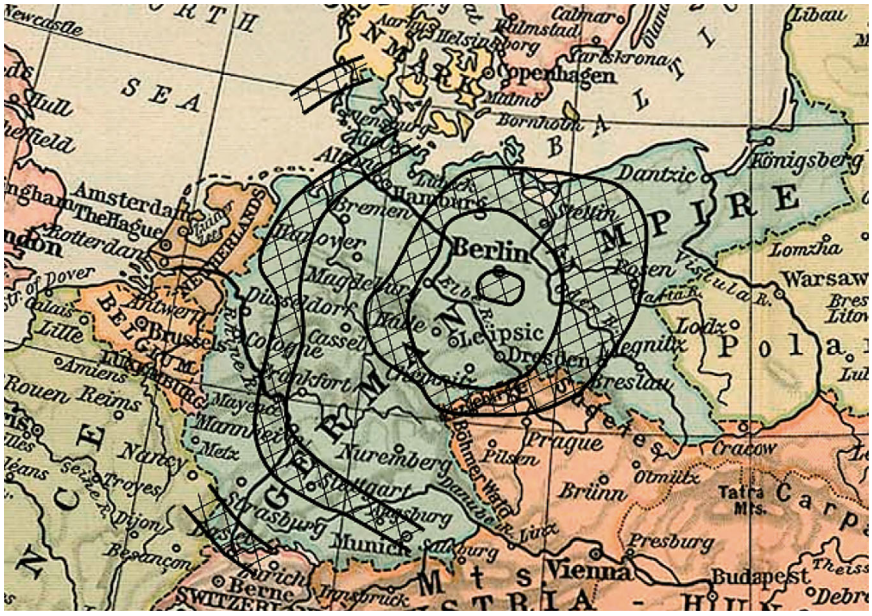

FIGURE 6 | Areas in the old German Empire where an explosion at Kummersdorf (south of Berlin) on December 18, 1925, has been heard. The cross-hatched regions in the map are those regions in which the explosion was heard. The ring-like structure with zones of audibility alternating with zones of silence suggested that the sound was reflecting from the ground and then being refracted back down to the ground over and over. The distance between rings suggested that the refraction was taking place in the stratosphere. (Reproduced from T. B. Gabrielson, "Refraction of sound in the atmosphere," Acoustics Today, ref. [6], with permission of Acoustical Society of America. Copyright 2006, Acoustical Society of America, and with permission of the author. The image in ref. [6] was adapted from B. Gutenberg, Handbuch der Geophysik, where the base map had been used by permission from The Historical Atlas by William R. Shephard, 1911.)

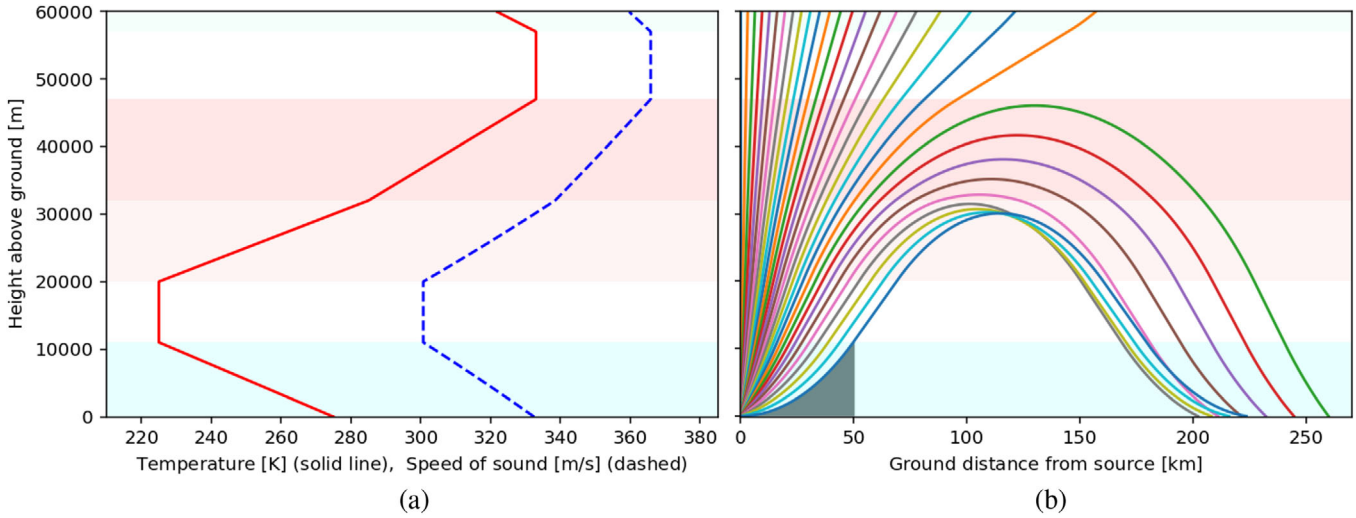

FIGURE 7 | (a) Temperature and speed of sound profiles at increasing altitude in the medium, according to a piecewise linear approximation of the winter temperature profile reported in ref. [6] and by assuming the atmosphere is made of ideal, dry air. (b) Ray tracing of a source at zero altitude in the given atmosphere. The polar angle of the initial ray direction $\mathbf{t}$ is varied between 0° and 90°, with a constant step of 3. Note that the polar axis is the vertical line at the source position, pointing to positive altitudes. The zone of silence due to the zero-altitude speed-of-sound gradient is marked in gray, limited to the troposphere.

temperature profile, the model predicts a zone of audibility at a ground distance between 200 and 250 km from the source. This qualitatively agrees with the experimental result observed for the 1925 explosion and justifies the existence of alternating rings of audibility and silence on the ground through stratosphere refraction and ground reflection.

5 | Conclusions

The refraction law, also known as Snell's law, had to be discovered at least three times before finding its way into the common knowledge of the current scientific community. We presented a model based on the linear expansion of the refraction law, which

can be successfully used to trace curvilinear sound paths in a medium with an inhomogeneous wave velocity field. In such a medium, the wavefronts have curvature radii, which are no more directly related to the distance traveled from the source. The present model enables the determination of the curvature evolution in the vicinity of the ray through the numerical integration of Equations (11) and (13), whose determination and numerical evaluation are detailed in ref. [5]. The numerical evaluation of the ray paths for sound radiation in a stratified model of the atmosphere was also developed in ref. [5]. We applied the model to reproduce the audibility pattern on the ground of a 100-year-old experiment about the sound field at observation points in the German Empire, due to an explosion in a firing range by Berlin. By using a piecewise linear temperature distribution profile for increasing altitude in the atmosphere, the model qualitatively reproduces the distribution of alternating ring-shaped audibility and silence patterns on the ground, see Figure 7. The model verifies the fact that the explosion was not heard in Frankfurt Oder and was audible in Poznan, in spite of Poznan being located at a greater geodesic distance from the explosion site. This is due to the refraction in the stratosphere, where we assumed particularly high temperatures.

Acknowledgments

This work has been a mix of positive and very sad feelings. Oskar Bschorr has been the principal motivator in the initial development and in the publication of the present theory at the annual conference of the GAMM. I wish I had met him in person there, I am sure he would have enjoyed the scientific discussions and seeing one of the team "planting" a tree.

Endnotes

[1] Note that this is a deduction of the first author, based on the information in Figure 6 and on his travel by train to attend the GAMM conference, including a displacement between Berlin and Poznan. By looking at the map reported in Figure 6, the city of Poznan, indicated in the map with the old German name Posen, is in the audible-explosion area, while Frankfurt Oder, located between the explosion site and Poznan, in the vicinity of the river Oder, is in a region where sound was not heard.

References

1. K. Hentschel, "Das Brechungsgesetz in der Fassung von Snellius: Rekonstruktion seines Entdeckungspfades und eine Übersetzung seines lateinischen Manuskriptes sowie ergänzender Dokumente," *Archive for History of Exact Sciences* 55, no. 4 (2001): 297–344.

2. J. Lohne, "Thomas Harriott (1560–1621)," *Centaurus* 6, no. 2 (1959): 113–121.

3. R. Rashed, "A Pioneer in Anaclastics: Ibn Sahl on Burning Mirrors and Lenses," *Isis* 81, no. 3 (1990): 464–491.

4. O. Bschorr, "Bestimmung von Wellenpfaden via Snellius-Brechungsgesetz. OneWay-Wellengleichung," in *Fortschritte der Akustik - DAGA 2024* (Deutsche Gesellschaft für Akustik e.V., DEGA, 2024).

5. O. Bschorr and A. Bassetti, "Ray Tracing via Snellius," *Journal of Sound and Vibration* 621 (2026): 119398.

6. T. B. Gabrielson, "Refraction of Sound in the Atmosphere," *Acoustics Today* 2, no. 2 (2006): 7–17.

7. A. Pierce, *Acoustics —An Introduction to Its Physical Principles and Applications* (Acoustical Society of America, 1991).

8. International Civil Aviation Organization, ICAO, "Manual of the ICAO Standard Atmosphere, Extended to 80 Kilometres," Technical Report Doc 7488/3 (ICAO, 1993).